# Accepted Manuscript


Towards a better comprehension of interactions in the crystalline N-acetylbenzylamine and its sulphur analogue N-benzyl-ethanethioamide. IR, Raman, DFT studies and Hirshfeld surfaces analysis

Wioleta Edyta Śmiszek-Lindert, Elżbieta Chełmecka, Olaf Lindert, Anna Dudzińska, Ilona Kaczmarczyk-Sedlak

| | |
|---|---|
| PII: | S1386-1425(18)30411-6 |
| DOI: | doi:10.1016/j.saa.2018.05.021 |
| Reference: | SAA 16044 |
| To appear in: | *Spectrochimica Acta Part A: Molecular and Biomolecular Spectroscopy* |
| Received date: | 12 March 2018 |
| Revised date: | 2 May 2018 |
| Accepted date: | 6 May 2018 |

Please cite this article as: Wioleta Edyta Śmiszek-Lindert, Elżbieta Chełmecka, Olaf Lindert, Anna Dudzińska, Ilona Kaczmarczyk-Sedlak , Towards a better comprehension of interactions in the crystalline N-acetylbenzylamine and its sulphur analogue N-benzyl-ethanethioamide. IR, Raman, DFT studies and Hirshfeld surfaces analysis. The address for the corresponding author was captured as affiliation for all authors. Please check if appropriate. Saa(2017), doi:10.1016/j.saa.2018.05.021

# Towards a better comprehension of interactions in the crystalline N-acetylbenzylamine and its sulphur analogue N-benzyl-ethanethioamide. IR, Raman, DFT studies and Hirshfeld surfaces analysis

Wioleta Edyta Śmiszek-Lindert[a1], Elżbieta Chełmecka[b], Olaf Lindert[c], Anna Dudzińska[d], Ilona Kaczmarczyk-Sedlak[a]

[a] *Department of Pharmacognosy and Phytochemistry, Medical University of Silesia in Katowice, School of Pharmacy with the Division of Laboratory Medicine in Sosnowiec, Jagiellońska 4, 41-200 Sosnowiec, Poland*

[b] *Department of Statistics, School of Pharmacy with Division of Laboratory Medicine, Medical University of Silesia, 30 Ostrogórska Street, 41-200 Sosnowiec, Poland*

[c] *Clinic of Infertility Treatment, Gynecology and Obstetrics, Bocian Clinic in Katowice, Dąbrówki 13, 40-081 Katowice. Poland*

[d] *Institute of Building Materials and Structures, Faculty of Civil Engineering, Cracow University of Technology, 31-155 Cracow, Poland*

ABSTRACT

This paper presents the investigation results of the polarized IR spectra of the hydrogen bond in crystals of N-acetylbenzylamine and its sulphur analogue N-benzyl-ethanethioamide. The spectra were measured at 298 and 77 K by a transmission method, with the use of polarized light. The Raman spectroscopy, Hirshfeld surfaces analysis and DFT studies have been also reported. Theoretical calculations of the isolated molecule were performed by using density functional theory (DFT) method at B3LYP/6-311(d,p), B3LYP/6-311++G(d,p) and B3LYP/6-311++G(3df,2pd) basis set levels. The geometrical parameters of analyzed compounds are in good agreement with the XRD experiment. The vibrational frequencies were calculated and subsequently values have been compared with the experimental Infrared and Raman spectra. It has been shown that the observed and calculated frequencies are found to be in good agreement, as well as the analysis of the Hirshfeld surface has been well correlated to the spectroscopic studies. Additionally, the highest occupied molecular orbital energy ($E_{HOMO}$), lowest unoccupied molecular orbital energy ($E_{LUMO}$), the energy gap between $E_{HOMO}$ and $E_{LUMO}$ ($\Delta E_{HOMO–LUMO}$), molecular electrostatic potential and global reactivity descriptors *viz.* chemical potential, global hardness and electrophilicity have been calculated. In N-acetylbenzylamine the presence of the N-benzylamide fragment is essential for activity.

[1] Corresponding author
E-mail address: wlindert@sum.edu.pl; wiola.lindert@wp.pl (W.E. Śmiszek-Lindert)

*Keywords:* IR and Raman spectra; Hydrogen bond; Hirshfeld surfaces; DFT calculations; HOMO and LUMO

## 1. Introduction

Epilepsy is a syndrome of different cerebral disorders of the central nervous system (CNS), which affects 2.4 million people of the world each year [1, 2]. The majority of epileptic disorders are not self-limiting over time, and therefore require a long-lasting and often even lifelong antiepileptic drug (AED) treatment. This disease becomes particularly problematic for women of childbearing age. According to the literature data, 50% of women with epilepsy suffer from dysfunctions such as oligomenorrhea, amenorrhea, abnormally shortened or lengthened menstrual cycles, polycystic ovaries (PCO; refers to an ultrasound scan image) or polycystic ovary syndrome (PCOS) [3]. In turn, the pregnant women with epilepsy are understandably anxious about pregnancy, especially in view of the influence of their disease on course of pregnancy and the possible impact of the antiepileptic therapy on child as well as her. Studies on placental transfer of AEDs during the first (12 weeks) and second trimester (weeks 13-27) of human pregnancy are still very deficient.

Antiepileptic drugs belong to many different chemical classes of compounds, and therefore the choice of AEDs for a patient depends upon the individual factors as e.g. type of syndrome, coexisting diseases or age [4, 5]. Besides, nearly 30% of these patients are not well controlled by a single antiepileptic drug and usually require treatment with a combination of two or more AEDs. The classical AEDs like phenobarbital, primidone, ethosuximide, phenytoin, valproate, and benzodiazepine, are widely used in ambulatorium and clinical practice, nevertheless have a range of side effects [6-8]. It should be noted that several new compounds such as zonisamide, vigabatrin, gabapentin have appeared next the wide use of another traditional antiepileptic drugs such e.g. valproic acid or carbamazepine [5, 9]. In recent years, many newer antiepileptic drugs have been investigated as add-on therapy for partial epilepsy (partial on-set seizures). Among these drugs are retigabine (ezogabine), losigamone or ganaxolon which now is being evaluated in clinical trials [10, 11].

The search for new anticonvulsant drugs still continues to be an active area of study in medicinal chemistry, and the need to synthesize newer compounds is desirable to treat those cases that are resistant to the available drugs as well as to reduce the side effects to the lowest possible level [12]. Malawska et *al*. [6] based on the results of pharmacological, physicochemical, roentgenostructural and molecular modelling investigations of new anticonvulsant derivatives of α-substituted N-benzylamides of γ-hydroxy- and γ-acetoxybutyric acid (GHB) determined the pharmacophore model. It has been shown that the N-benzylamide moiety is essential structural unit for activity of new anticonvulsant compounds. And secondly, all active amides should include another hydrophobic fragment (aryl ring) as a distal binding site and also a hydrogen bonding domain; Scheme 1. [6].

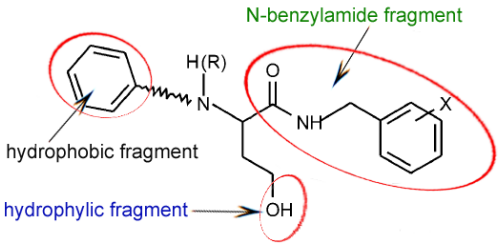


Scheme 1. Pharmacophore model for anticonvulsant of α-substituted N-benzylamides of γ-hydroxybutyric acid.

Hydrogen bonds (H-bonds) are very important interactions which are necessary for activity of anticonvulsants. So far, correlation has been not demonstrated between the strength of hydrogen bonding and the type or extent of anticonvulsant action [13]. Generally, this kind of interactions is based on an electrostatic interaction between the nonbonding electrons of a heteroatom (e.g., O, N, S) and the electron-deficient hydrogen atom of a molecular group, most often N-H, O-H or S-H. Hydrogen bonds are strongly directional, having energies ranging from 1 to 10 kcal/mol (weak H-bonds $|\Delta H| < 20$ kJ/mol; intermediate H-bonds 20 kJ/mol $< |\Delta H| <$ 40kJ/mol; strong H-bonds $|\Delta H| > 40$ kJ/mol [14]). It is well-known, that the hydrogen bonds play key and even fundamental role in molecular biology. They are

responsible for the stability, formation and for the functioning of many biomolecules and supramolecules. H-bonds are also important for molecular recognition and thus will not only determine a compound's activity but either its metabolism or transport properties [15, 16].

In the present study we have chosen structurally related compound to the N-benzylamide fragment of new anticonvulsant derivatives [6], having the only methyl group connected with the carbon atom of amide bond (–CO–NH–): N-acetylbenzylamine. This choice is not accidental, because subsequent studies demonstrated the importance of the acetamido fragment ($R^1$= CO-$CH_3$) for potent anticonvulsant activity and showed that either a decrease (i.e. $R^1$=CO-H) or increases (i.e. $R^1$=CO-$CH_2$-$CH_3$, -CO-CH-$(CH_3)_2$, -CO-C-$(CH_3)_3$) in the size of this moiety led to reduced activity. Moreover, when the acetamido group ($CH_3$CO-NH) was replaced with methyl, methoxy, hydroxy, acetoxy, or halogen then compounds were characterized with diminished anticonvulsant activity [17]. Additionally, N-acetylbenzylamine is also key intermediate in the preparation of various therapeutic small molecules, like maphenide; (N-aminomethyl)-benzenesulfamide [18]. This drug belong to the group of sulfonamide drugs which in combination with pyrimethamine or trimethoprim are active with respect to a few protozoal infections, including *Toxoplasma*, *Plasmodium falciparum*, and *Pneumocystis carinii* [18].

In this paper we combine the results of the spectral measurements - IR and Raman, Hirshfeld Surfaces (HS) computational method and DFT quantum chemical calculations focusing on a verify and to investigate of the existing interactions in the crystal lattice of N-acetylbenzylamine. We investigate the role of the main intermolecular interactions on stabilization of its structure. For a better understanding of the hydrogen bonds role, the oxygen by sulphur in amide bond of N-acetylbenzylamine has been replaced, giving of N-benzyl-ethanethioamide. This modification has been thought to have an enhanced or reduced effect on the conformational flexibility or binding affinity, depending on steric or hydrogen

bonding strength [19]. Additionally, the various reactivity and selectivity descriptors such as electrophilicity index ($\omega$), chemical potential ($\mu$) and global hardness ($\eta$) have been calculated. It should be mentioned that the value of the $\omega$ describes the biological activity of a molecule.

## 2. Experimental Section

### *2.1. Materials and physical measurements*

N-acetylbenzylamine (**1**) and N-benzyl-ethanethioamide (**2**) have been synthesized by Śmiszek-Lindert - the description of this procedure was presented in the papers [20, 21]. The XRD structural studies were performed by Śmiszek-Lindert and *al* [20, 21].

The FT-IR spectra of the title compounds powdered in KBr pellet as well as their polarized IR spectra (single crystals) have been recorded on a FT-IR Nicolet Magna 560 spectrometer. All spectra were accumulated with a spectral resolution of 2 $cm^{-1}$ and recorded by accumulating of 32 scans. The spectra have been collected in the 4000-400 $cm^{-1}$ range. In turn, spectral experiment in the case of polycrystalline samples have been performed at temperature 298K, while the IR spectra of the monocrystalline samples were measured at two temperatures, 298K and 77K. The single crystals of (**1**) and (**2**) have been obtained by crystallization from a melted substance (melting point of compound (**1**) and (**2**) is 333K [20] and 338-339K [21], respectively), which appears between two closely $CaF_2$ windows. The details of the experimental techniques of the preparing and the selection of single crystals from a mosaic are given in References [22-26]. Measurements of the spectra of monocrystalline fragments have been performed for two different orientations of the electric field vector *"E"* (polarization 0° and 90°).

Raman measurements have been performed using a WITec confocal CRM alpha 300 Raman microscope. The spectrometer was equipped with an air-cooled solid state laser

operating at 532 nm and CCD detector, cooled to 203K. The laser was coupled to the microscope via a 50 μm diameter optical fiber. A dry Olympus LM PLAN FJ (50×/0.5; ∞/0) objective has been used. The integration time for a single spectrum was 0.5 s and the spectral resolution equalled 3 $cm^{-1}$. Raman spectrum has been measured in the range 4000-120 $cm^{-1}$. Raman measurements and data analyses have been performed using WITec software (Project FOUR 4.1) [27].

*2.2. Hirshfeld Surface (HS) analysis*

For analysis of the intermolecular interactions in the crystal lattice of the N-acetyl-benzylamine and N-benzyl-ethanethioamide the Hirshfeld Surface method has been also used. This tool is based on the calculation of the promolecular electron density both crystal and in gas phase, and provides a convenient means of quantifying the interactions within the crystal structures, revealing significant similarities and differences between related structures by individuate the packing motifs. To obtain the fingerprint plots the CrystalExplorer program [28] has been used. The fingerprint plots are generated based on the $d_e$ and $d_i$ distances, the distance from the HS to the nearest nucleus outside and inside the surface, respectively. The 2-D fingerprint plots have been also used for visualizing, exploring and quantifying intermolecular interactions.

*2.3. Quantum chemical calculations*

Theoretical calculations have been carried out using B3LYP density functional theory. In calculations for (**1**) and (**2**) compound the 6-311(d, p), 6-311++G(d, p) and 6-311++G(3df, 2pd) basis sets were used [29, 30]. All quantum-mechanical calculations were performed using the GAUSSIAN 09 program [31]. Herein, it is also important to note that all computations have been carried out in gas phase. The harmonic vibrational wavenumbers and intensities were calculated at the same level of theory.

In order to understanding of the chemical reactivity and site selectivity of the molecular systems has been used the conceptual DFT, which is a subfield of DFT [32, 33]. The various reactivity and selectivity descriptors such as chemical potential ($\mu$), global hardness ($\eta$) and electrophilicity index ($\omega$) have been calculated [34, 35]. It should be noted that the electrophilicity index is a very important descriptor, which defines a quantitative classification of global electrophilic nature of a molecule within a relative scale. Value of the $\omega$ describes the biological activity of a molecule. This descriptor has been defined by Parr et al. and is expressed as $\omega = \mu^2/2\eta$ [36]. The $\mu$ and $\eta$ have been calculated by using Koopmans' theorem [35]: $\mu = E_{LUMO} + E_{HOMO}/2$; $\eta = E_{LUMO} - E_{HOMO}/2$ where $E_{LUMO}$ and $E_{HOMO}$ (correspond to the Kohn–Sham [37]) is the lowest unoccupied and the highest occupied molecular orbital's energy, respectively. It is worth noting, that the $\mu$ and $\eta$ are associated with the charge transfer ability of the molecule in its ground state and with the resistance of the molecule to exchange electronic charge with the environment in its ground state, respectively.

## 3. Results and Discussion

### *3.1. IR and Raman spectral studies*

Herein, we start our investigation from spectroscopic studies. In Fig. 1 (a) and (b) has been shown the molecular structure of N-acetylbenzylamine and N-benzyl-ethanethioamide, respectively. The FT-IR and Raman spectrum of polycrystalline sample of (**1**) and (**2**) compound measured with the use of the KBr pellet technique at room temperature (298K) has been shown in Fig. 1 (c) and (d), respectively. In Fig. 1 (c) and (d), there is also drawn the Raman spectrum of a polycrystalline samples indicating location of the ν(CH) bands. The polarized IR spectrum of (**1**) and (**2**) compound single crystals measured at 77K is illustrated in Figure 2 (a) and (c), respectively. In turn, the temperature-dependence of the polarized crystalline spectra of the same crystals has been presented in Figure 2 (b) and (d).

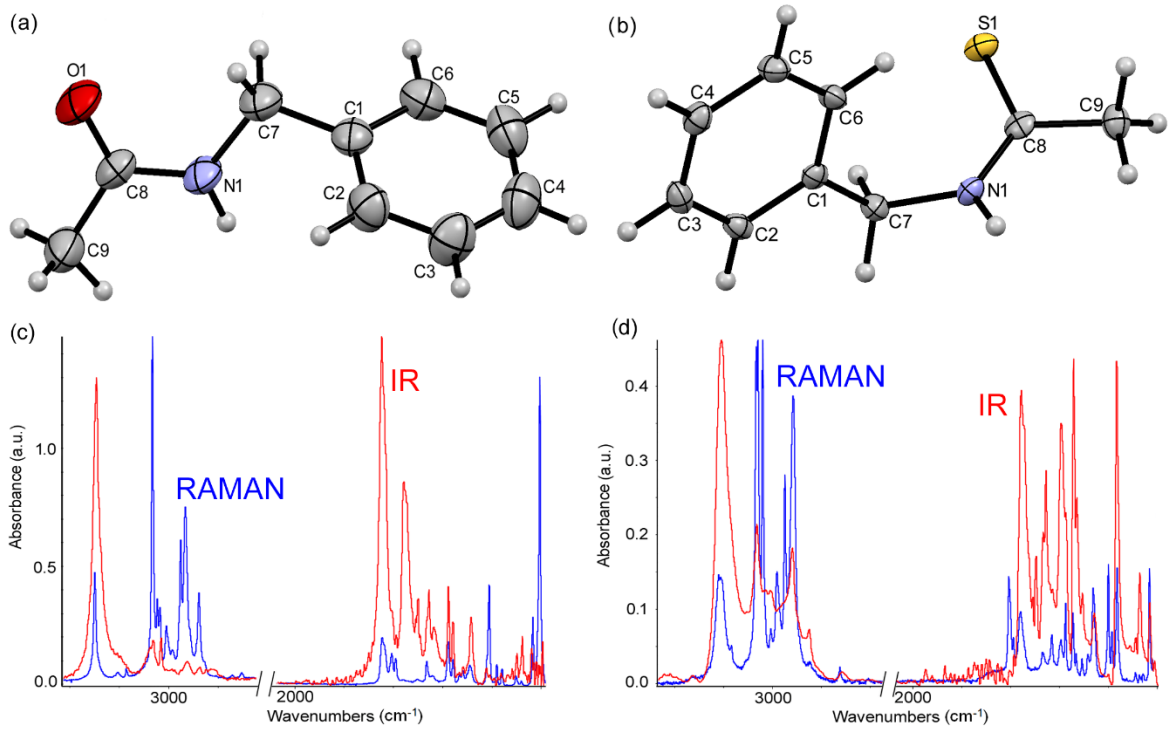


**Fig. 1.** ORTEP view and atom numbering scheme of N-acetylbenzylamine (a) and N-benzyl-ethanethioamide (b) with displacement ellipsoid at the 50 % probability level. H atoms are shown as small spheres of arbitrary radius. The IR spectra of polycrystalline samples of **1** (a) and **2** (b) measured at 298 K by the KBr pellet technique with the Raman spectra for identification of the C–H bond vibration lines.

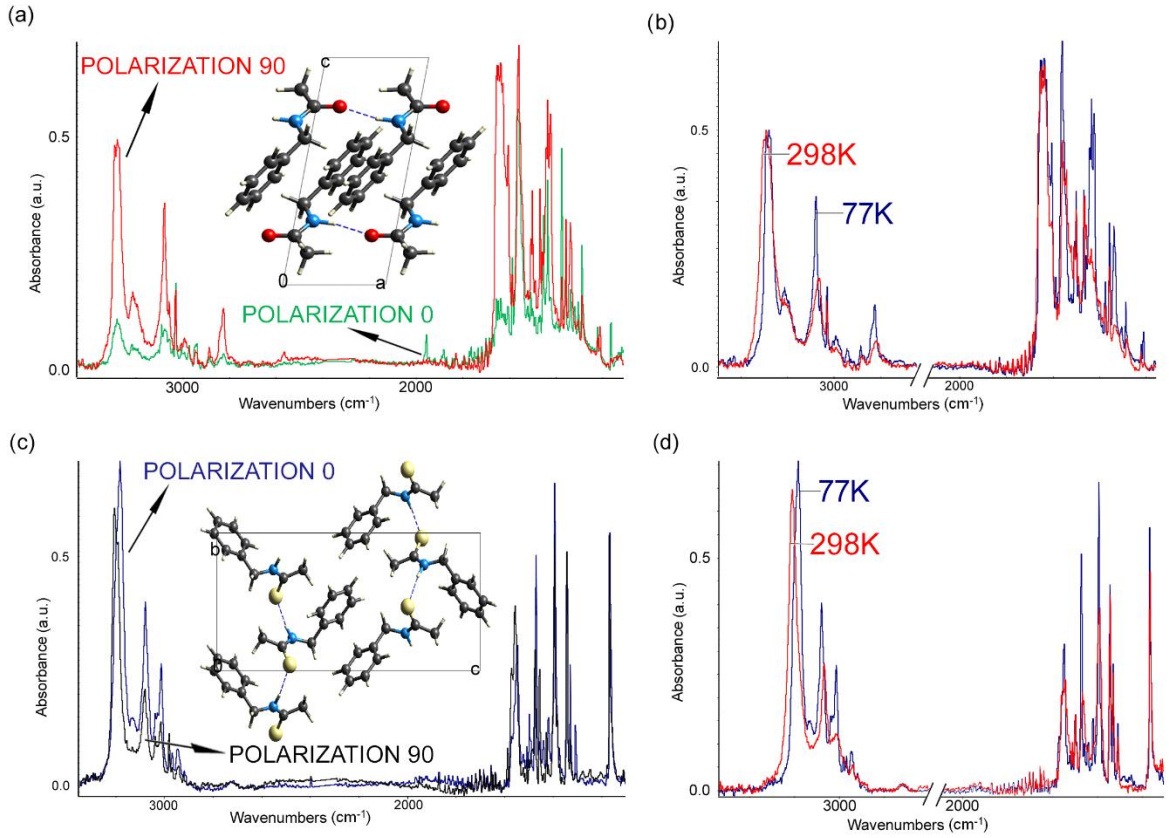


**Fig. 2.** Polarized spectra of a single crystal of (**1**) (a) and (**2**) (c) measured at 77 K with the packing diagram of (**1**) and (**2**) viewed along the *b* and *a* axis, respectively (inset). Temperature effect in the polarized spectra of a single crystal of N-acetylbenzylamine (b) and N-benzyl-ethanethioamide (d).

Based on analysis of crystallographic data we can conclude that molecules of analyzed compounds in the crystal lattices are connected by N-H···O moderate (**1**) and N-H···S weak (**2**) framework of intermolecular hydrogen bonds. The strength of these H-bonds has been also confirmed by our IR studies. In the case of polycrystalline N-acetylbenzylamine the vibrations can be divided into following main types: N-H stretching band (~3294 $cm^{-1}$), C=O stretching band (amide I band; ~1639 $cm^{-1}$), N-H bending (amide II band; ~1559 $cm^{-1}$), C-N stretching band (amide III band; ~1373 and 1362 $cm^{-1}$), and aromatic C-H stretching in the region ~3087–2972 $cm^{-1}$); see Fig. 2 (c). From Fig. 1 (c) can be also see that the ν(NH) band is strong, whereas the ν(CH) bands are weak. In contrast to the IR spectrum, the Raman

spectrum shows strong ν(CH) bands, corresponding to C–H bond stretching vibrations in N-acetylbenzylamine molecules and relatively weak ν(NH) bands. These spectral effects seem prove a partial covalent character of the N–H bonds. In turn, further analysis of IR spectrum of monocrystalline N-acetylbenzylamine indicate a strong and relatively narrow band extending over the frequency range ~3371–2950 $cm^{-1}$ (Fig. 2 (a)). This region and essential features of the band prove the presence of the intermolecular N-H···O interactions in the crystal lattice of (**1**). A part of the molecular framework of the analyzed amide, viewed along the *b* axis, demonstrating the hydrogen-bonded chains has been shown in Fig. 2 (a) (inset picture). As shown, the ν(NH) band in the spectra of N-acetylbenzylamine crystals is characterized by the two-branch structures. This two-branch ν(NH) band has different integral intensities, the longer-wave branch (~3160-2950 $cm^{-1}$) is characterized by relatively low intensity in contrast to the shorter-wave branch (~3400-3160 $cm^{-1}$). In the next step, we carried out thorough spectral measurements with the use of polarizer. The IR spectra of monocrystalline samples (see Fig. 2(a)), measured at the different orientation of the electric field vector *"E"*, the incident light on the crystal, showed a large variability of some bands intensity. The polarized light especially strongly influences the intensity of bands of the N-H bonds stretching vibrations in the molecules of (**1**). It has been observed that the most intense polarized component of the crystal spectrum of the (**1**) has been measured on the electric field vector (*"E"*) perpendicular to the direction of the chains of the intermolecular interactions N-H···O in the crystal lattices (polarization 90º). Whilst, a weaker polarized component of the analyzed bands has been noticed for the parallel orientation of the *"E"* (polarization 0º). It can be also seen that the shorter-wave and the longer-wave branch of $\nu_{N-H}$ band proportionally changes the intensity. It was further found that the polarization effects are also visible in the some bands lying at the lower frequencies.

Having outcome of these investigations in mind, we carried out analogical studies for N-benzyl-ethanethioamide. In this case the IR spectrum of polycrystalline N-benzyl-ethanethioamide (see Fig. 1 (c)) exhibits the presence of following main bands: ν(NH) band at ~3213 $cm^{-1}$, the band at 1392 $cm^{-1}$ which is attributed to ν(CN) vibration modes, as well as bands occurring in the range of ~1570-1514 $cm^{-1}$ originating from the C=S stretching frequency. The ~3300-2850 $cm^{-1}$ region and essential features of the band prove the presence of the intermolecular N-H···S interactions in the crystal lattice of (**2**). When analyzing polarization properties of the crystal spectra of N-benzyl-ethanethioamide, measured in the frequency range of the ν(NH) band, one can find that also in these case the polarization effects are being identifiable (see Fig. 2 (c)). The polarized IR spectra, showed that ν(NH) band is characterized by the two spectral branches, and this doublet component differ by its relative intensities. It has been observed that the intense polarized component has been measured on the electric field vector (*"E"*) parallel to the direction of the chains of the intermolecular interactions N-H···S in the crystal lattices (polarization 0º). Whilst, a weaker polarized component of the ν(NH) band has been noticed for the perpendicular orientation of the *"E"* (polarization 90º). It was found that the shorter-wave branch of ν(NH) band (~3300-3120 $cm^{-1}$) is of higher intensity than that of the spectral branch intensity of the longer-wave range (~3120-2850 $cm^{-1}$). Herein, just to mention that the studies of the polarized IR spectra of the molecular crystals of N-acetylbenzylamine and N-benzyl-ethanethioamide for spatially oriented lattices of the hydrogen bonds are the source of a complete data system concerning the *inter*-hydrogen bond interactions. Besides, the IR spectroscopy of hydrogen bonded molecular crystals in polarized light seems to be a most promising experimental method for studying diverse aspects of inter-hydrogen bond interactions. Measurements of the polarized IR spectra of spatially oriented hydrogen bond systems, in the lattices of molecular crystals, can deliver data, allowing estimating the vibrational transition moment directions to the

excited states of the proton vibrations in the crystals, as well as the symmetry of the proton vibration exciton states [38].

Further our spectral experiment show that, with temperature decreases, a noticeable change in the intensity of the ν(NH) band has been observed. In the case of (**1**) the intensity of the longer-wave branch considerably grows, while the intensity of the band shorter-wave branch remain practically unchanged; see Fig. 2 (b). In turn, for N-benzyl-ethanethioamide the integral intensities of the long- and the short-wave branches of the ν(NH) bands are characterized by relatively growth (Fig. 2 (d)).

Herein, it should be added that various quantities characterizing H-bonds of (**1**) and (**2**) have been described below in the section *DFT calculations*.

*3.2. Hirshfeld Surfaces (HS) analysis*

In the next step, we performed analysis molecular interactions with the use of Hirshfeld Surfaces (HS) technique. Figure 3 shows the intermolecular contacts between the molecules of the title compounds *via* Hirshfeld Surfaces analysis. Figure 4 (h-i) and 5 (g-h) presents the molecular Hirshfeld Surface, which has been mapped over $d_{norm}$ (normalized contact distance) range from -0.536 to 1.043 Å for (**1**) and -0.345 to 1.150 Å for (**2**). In turn, the fingerprint plots of (**1**) and (**2**) have been showed in Fig. 4 (a-g) and Fig. 5 (a-f), respectively, with view of the three-dimensional HS mapped with $d_{norm}$.

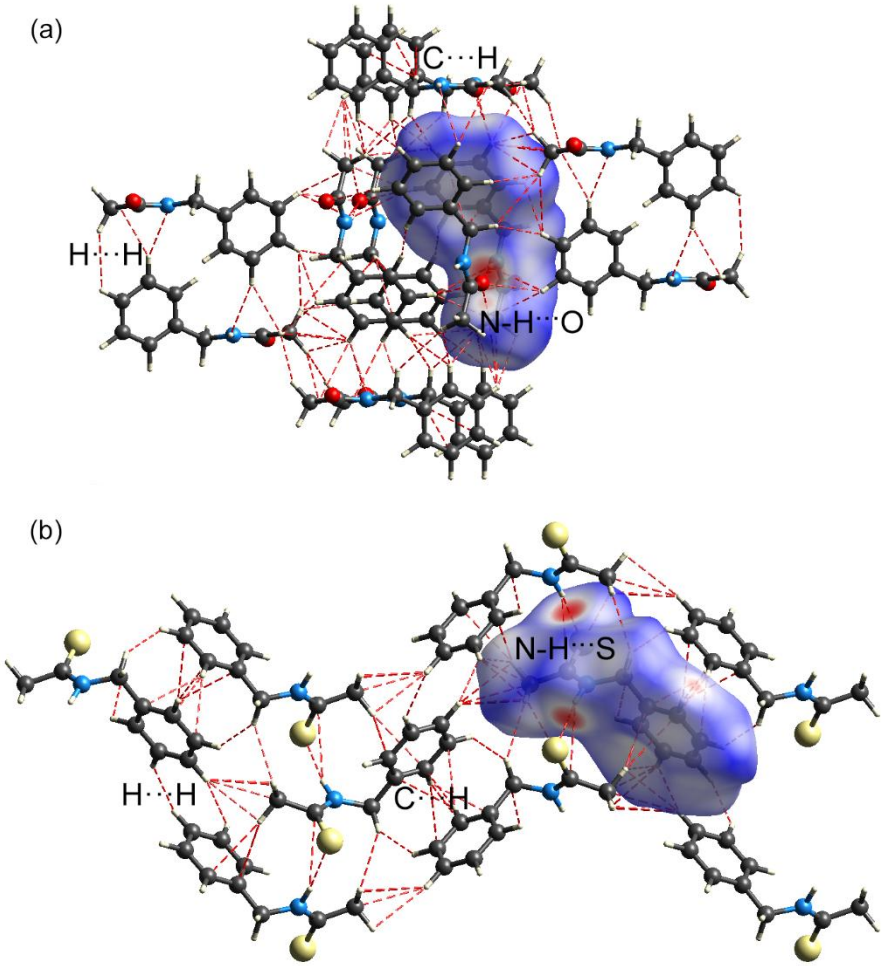


**Fig. 3.** Hirshfeld surfaces mapped with $d_{norm}$ and part of the crystal structure of (**1**) (a) and (**2**) (b) showing the selected intermolecular interactions.

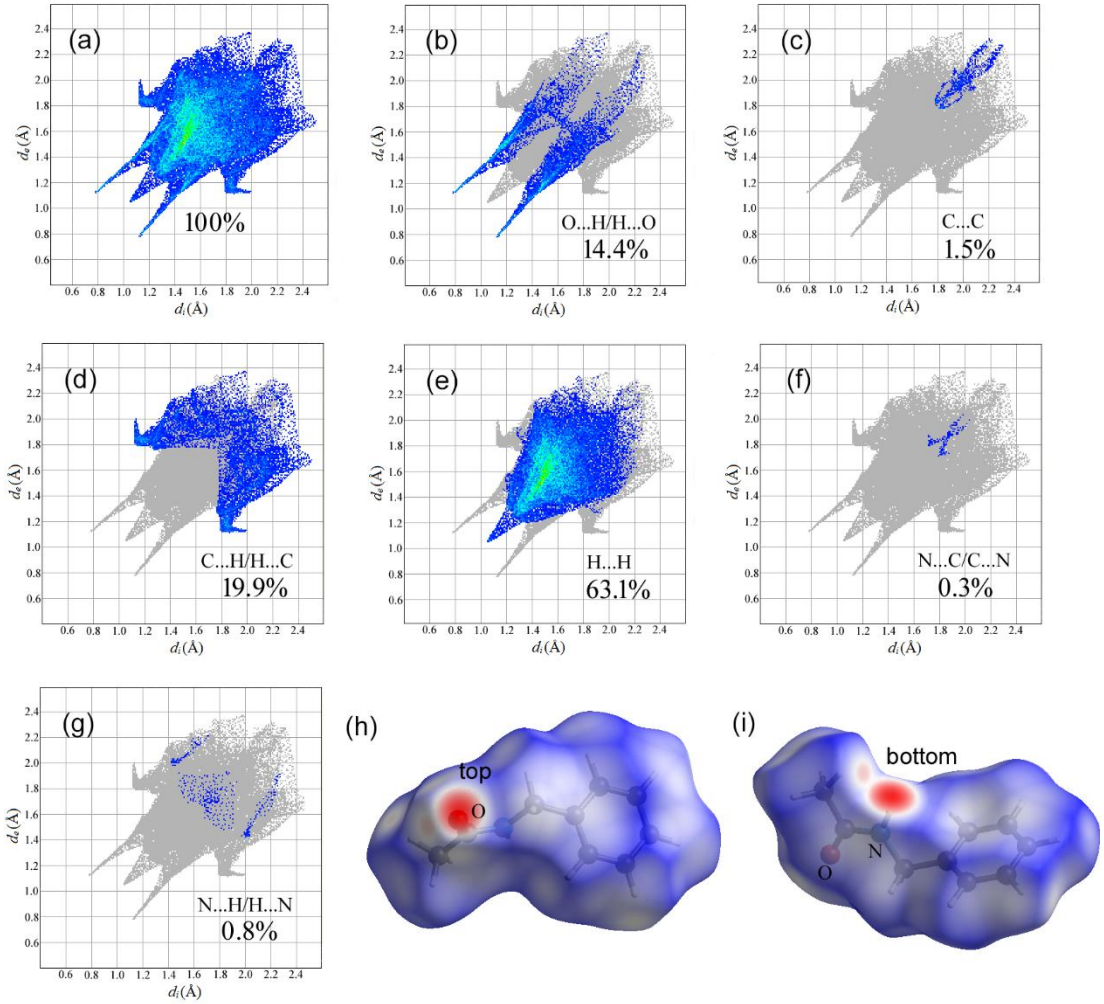


**Fig. 4.** (a-g) The two-dimensional fingerprint plots of N-acetylbenzylamine, showing all interactions ($d_e$ and $d_i$ represent the distances from a point on the HS to the nearest atoms outside (external) and inside (internal) the surface, respectively). (h) and (i) View of the three-dimensional Hirshfeld surface (HS) of (**1**) mapped with $d_{norm}$ (top and bottom view of the molecule). Colour scale is between -0.536 au (red) and 1.043 au (blue).

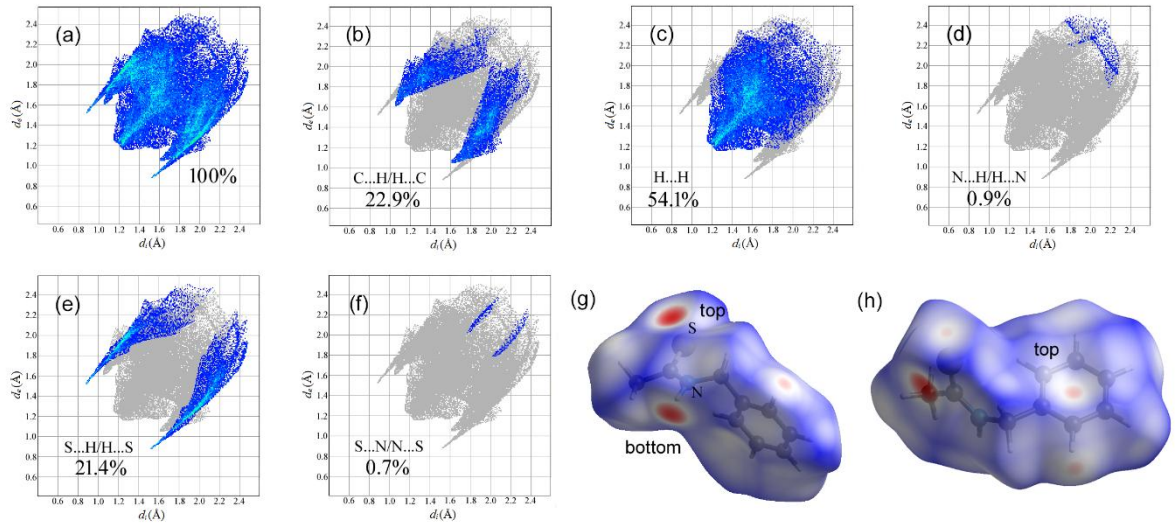


**Fig. 5.** (a-f) The two-dimensional fingerprint plots of N-benzyl-ethanethioamide, showing all interactions ($d_e$ and $d_i$ represent the distances from a point on the HS to the nearest atoms outside (external) and inside (internal) the surface, respectively). (g) and (h) View of the three-dimensional Hirshfeld surface (HS) of (**2**) mapped with $d_{norm}$ (top and bottom view of the molecule). Colour scale is between -0.345 au (red) and 1.150 au (blue).

As shown in Fig. 4 (h-i) and Fig. 5 (g-h) the large circular depressions (deep red), which are visible on the front and back views of the surface are indicative of the hydrogen bond contacts N-H···O and N-H···S, respectively. To get a better analysis on the detailed structures we turn to a comparison of the fingerprint plots. In the case of N-acetylbenzylamine the H···O/O···H interactions are represented by a pair of symmetrical large sharp spikes with the shortest distribution points in the fingerprint plots in the region of $d_i$ = 1.12 Å, $d_e$ = 0.79 Å and $d_i$ = 0.79 Å, $d_e$ = 1.12 Å for left (upper area; acceptor) and right (bottom region; donor), respectively (see Fig. 4 (b)). The H···O/O···H intermolecular contacts comprise 14.4%. While, N-benzyl-ethanethioamide is characterized by significantly more H···S/S···H contacts (21.4%) which are involved in hydrogen bonding. These contacts appear as a pair of symmetrical sharp spikes with the shortest distribution points in the fingerprint plots in the region of $d_i$ = 1.50 Å, $d_e$ = 0.86 Å and $d_i$ = 0.86 Å, $d_e$ = 1.50 Å for left (upper area; acceptor) and right (bottom area; donor), respectively (see Fig. 4 (e)). Herein, it should be also noted that the

complementary regions are observable in the 2-D fingerprint plots where one molecule acts as a donor ($d_e > d_i$) and the other as an acceptor ($d_e < d_i$) [39].

To answer the question, what interactions additionally stabilize the structure of (**1**) and (**2**), we have carried out further analysis of HSs. The other visible light-white regions in the $d_{norm}$ surfaces of (**1**) and (**2**) compounds are clearly indicative of weaker as well as longer contacts other than hydrogen bonds *viz*. H···H interactions. In the case of (**1**) the H···H interactions comprise 63.1% of the total Hirshfeld Surface area, and the 2-D fingerprint plot illustrates a large surface of scattered points (see Fig. 4 (e)). Interestingly, the contribution of H···H interactions to the Hirshfeld Surface decrease up to well 54.1% in (**2**); Fig. 5 (c). Worth emphasizing is the fact that, these results for (**1**) and (**2**) clearly demonstrate the important role of H···H contacts in stabilizing the molecular structure. Other significant interactions, which have been observed, are H···C contacts. The H···C/C···H intermolecular interactions comprise 19.9% for (**1**) and 22.9% for (**2**) of the total HS and represent two characteristic wings (see Fig. 4 (d) and Fig. 5 (b), respectively). This is evidence that van der Waals forces exert an important influence on the stabilization of the packing in (**1**) and (**2**). From Fig. 4 (c), (f), (g) and Fig. 5 (d), (f) it can be also seen the interactions which are not significantly important in the crystal structure of the title compounds.

The next step was to analyze the graphical scheme of the Molecular Electrostatic Potential (MEP). It should be noted that in theoretical models the Molecular Electrostatic Potential can characterize the induced electrostatic field [40]. The MEP has been mapped on Hirshfeld Surfaces using DFT/B3LYP method with 6-311G(d,p) basis set in the range of −0.093 a.u. to +0.155 a.u. for (**1**) and −0.063 a.u. to +0.138 a.u. for (**2**). The graphical scheme of the molecular electrostatic potential surfaces have been plotted by red region, which is a negative electrostatic potential (hydrogen acceptors) and by blue region, which is a positive electrostatic potential (hydrogen donor) (see Fig. 6 (a) and (b)). The N-acetylbenzylamine and

N-benzyl-ethanethioamide are polar molecules (μ=3.46 D and μ=5.37 D, respectively), but molecule of (**2**) has the higher value of dipole moment, and this has been reflected in the MEP. It was shown that carbonyl and thiocarbonyl group induces negative MEP, and thus is a candidate proton acceptor in hydrogen bond. Nevertheless, the region around the C=S group is more negative than observed for (**1**) around C=O group. In turn, the N-H group induces positive MEP. Thus, the hydrogen atom of N-H group may act as a hydrogen donor and also form a hydrogen bond. A MEP analysis also indicates that the above the benzene ring N-benzyl-ethanethioamide induces a more negative potential than benzene ring of N-acetylbenzylamine. This electronegative (red) patch is in contact with the weakly electropositive (blue) region around the methyl group and C-H group of benzene ring of neighboring molecule in the crystal lattice. Herein, it should be also stressed that previous studies indicates biologically active antiepileptic compounds exhibit lower MEP values in the environment of the oxygen atoms [40].

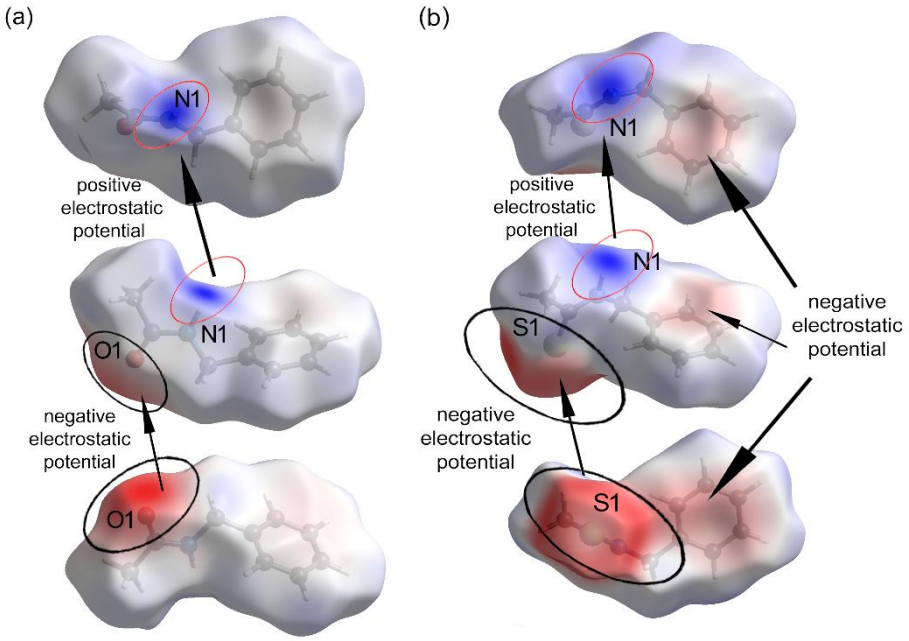

**Fig. 6.** Molecular Electrostatic Potential of (**1**) (a) and (**2**) (b) mapped on the Hirshfeld surface. Red region corresponds to negative electrostatic potential and blue to positive electrostatic potential.

Finally, the formation of the hydrogen bonds N-H···O and N-H···S in N-acetylbenzylamine and N-benzyl-ethanethioamide has also been substantiated by the DFT calculations.

*3.3. DFT calculations*

Theoretical studies have been started from the analysis of (**1**) and (**2**) geometric structure. Our studies indicate that both the use of B3LYP/6-311(d,p), B3LYP/6-311++G(d,p) as well as B3LYP/6-311++G(3df,2pd) level gives practically similar values of the geometrical parameters to the experimental ones. The experimental data on the geometric structure of (**1**) and (**2**) compound was compared with the calculated geometry parameters and have been listed in Table 1 and 2, respectively. View of the fact, that the calculated geometrical parameters showed a good approximation with the experimental data they became the basis for the calculating of the vibrational frequencies. The comparison of the calculated (B3LYP/6-311++G(3df,2pd)) IR and Raman spectrum of (**1**) and (**2**) with the experimental spectra has been presented in Fig. 7 (a)-(d). The calculated and experimental vibrational wavenumbers using B3LYP/6-311++G(3df,2pd) method have been shown in Table 3. It is also worth to stress that the vibrational wavenumbers obtained in the case of the DFT/B3LYP method with 6-311(d,p) and 6-311++G(d,p) basis set are similar to the vibrational wavenumbers received by 6-311++G(3df,2pd) basis set (data not shown).

Herein, it should be also noted that in the case of the computational values most of the optimized bond-lengths/angles are slightly shorter and longer than the experimental values. These small differences between the calculated and observed geometrical parameters can be assigned to the fact that the theoretical calculations were performed with the isolated

molecules in the gaseous phase while the experimental values have been based on the molecules in the solid state (crystalline state).

In Fig. 7 (a)-(d) one can observe that the difference between the experimental and theoretical ν(NH) band for (**1**) and (**2**) is clearly visible. In the case of experimental spectra the position of amine band is determined by intermolecular hydrogen bonding interactions between (−C(=O)−) and the NH group for (**1**) as well as (−C(=S)−) and the NH group for (**2**). From experimental IR spectrum of N-acetylbenzylamine (see Fig. 7 (a) – top panel) we see that the centre of ν(NH) band is shifted towards lower wavenumbers by about 221 $cm^{-1}$ with respect to the ν(NH) for theoretical spectrum (bottom panel). Its integrated intensity and widths is also greater than that of the corresponding ν(NH) of the same molecule establishing no H-bond (theoretical spectrum). As expected, these shift and widths also appear in Raman spectrum (see experimental and theoretical spectrum, Fig. 7 (c)). In turn, the integrated intensity of ν(NH) in Raman spectrum, in opposition to IR spectrum, is characterized by lower intensity. In the case of N-benzyl-ethanethioamide our IR and Raman results demonstrate analogous observations. As shown in Fig. 7 (b), the centre of ν(NH) band has been shifted towards lower wavenumbers by ~368 $cm^{-1}$ with respect to the ν(NH) for theoretical spectrum. As expected, we also observed increase of the integrated intensity and widths of ν(NH) band.

**Table 1** Comparison of selected calculated geometry parameters of N-acetylbenzylamine with the experiment.

| Experimental (XRD) [20] | | Theoretical DFT/B3LYP | | |
|---|---|---|---|---|
| | | 6-311(d,p) | 6-311++G(d,p) | 6-311++G(3df,2pd) |
| Bond lengths (Å) | | | | |
| C1-C2 | 1.385(14) | 1.397 | 1.397 | 1.395 |
| C2-C3 | 1.383(16) | 1.394 | 1.395 | 1.389 |
| C3-C4 | 1.367(16) | 1.392 | 1.393 | 1.390 |
| C4-C5 | 1.379(18) | 1.394 | 1.395 | 1.389 |
| C5-C6 | 1.375(16) | 1.392 | 1.392 | 1.391 |
| C6-C1 | 1.386(14) | 1.398 | 1.399 | 1.392 |
| C1-C7 | 1.505(14) | 1.519 | 1.518 | 1.521 |
| C7-N | 1.454(13) | 1.455 | 1.457 | 1.448 |
| N-C8 | 1.331(12) | 1.374 | 1.372 | 1.367 |
| C8-O | 1.233(10) | 1.218 | 1.222 | 1.219 |
| C8-C9 | 1.498(14) | 1.521 | 1.519 | 1.517 |
| Angles (°) | | | | |
| C1-C2-C3 | 120.92(10) | 120.73 | 120.73 | 120.82 |
| C2-C3-C4 | 120.15(11) | 120.05 | 120.04 | 120.04 |
| C3-C4-C5 | 119.73(11) | 119.61 | 119.62 | 119.53 |
| C4-C5-C6 | 120.15(12) | 120.24 | 120.23 | 120.31 |
| C5-C6-C1 | 121.00(11) | 120.53 | 120.54 | 120.53 |
| C6-C1-C2 | 118.04(10) | 118.83 | 118.83 | 118.76 |
| C5-C6-C1 | 121.00(11) | 121.04 | 121.00 | 120.05 |
| C2-C1-C7 | 120.70(9) | 120.11 | 120.15 | 119.16 |
| C1-C7-N | 111.11(8) | 112.76 | 112.55 | 115.21 |
| C7-N-C8 | 122.45(8) | 128.66 | 128.53 | 128.84 |
| N-C8-O | 122.90(9) | 120.81 | 120.73 | 120.63 |
| N-C8-C9 | 116.25(8) | 117.26 | 117.46 | 117.64 |
| O-C8-C9 | 120.84(8) | 121.92 | 121.81 | 121.73 |
| Dihedral angles (°) | | | | |
| C3-C2-C1-C7 | 179.49 | 177.93 | 178.02 | 177.97 |
| C5-C6-C1-C7 | 179.55 | -178.10 | -178.18 | -178.08 |
| C2-C1-C7-N | 128.62 | 139.46 | 135.38 | 157.21 |
| C6-C1-C7-N | -56.62 | -42.06 | -46.09 | -24.37 |
| C1-C7-N-C8 | 159.60 | 142.98 | 144.08 | 106.68 |
| C7-N-C8-O | -2.96 | 171.36 | 172.71 | -177.21 |
| C7-N-C8-C9 | 178.24 | -9.47 | -8.02 | 3.28 |

**Table 2** Comparison of selected calculated geometry parameters of N-benzyl-ethanethioamide with the experiment.

| Experimental (XRD) [21] | | Theoretical DFT/B3LYP | | |
|---|---|---|---|---|
| | | 6-311(d,p) | 6-311++G(d,p) | 6-311++G(3df,2pd) |
| Bond lengths (Å) | | | | |
| C1-C2 | 1.400(19) | 1.400 | 1.400 | 1.396 |
| C2-C3 | 1.397(2) | 1.391 | 1.392 | 1.389 |
| C3-C4 | 1.388(19) | 1.395 | 1.395 | 1.391 |
| C4-C5 | 1.390(2) | 1.392 | 1.392 | 1.389 |
| C5-C6 | 1.397(19) | 1.394 | 1.395 | 1.391 |
| C6-C1 | 1.394(19) | 1.396 | 1.397 | 1.393 |
| C1-C7 | 1.519(19) | 1.514 | 1.512 | 1.509 |
| C7-N | 1.467(17) | 1.464 | 1.468 | 1.465 |
| N-C8 | 1.323(17) | 1.347 | 1.349 | 1.345 |
| C8-S | 1.692(14) | 1.669 | 1.668 | 1.659 |
| C8-C9 | 1.507(2) | 1.510 | 1.510 | 1.506 |
| Angles (°) | | | | |
| C1-C2-C3 | 120.49(13) | 120.49 | 120.54 | 120.58 |
| C2-C3-C4 | 120.14(13) | 120.15 | 120.11 | 120.07 |
| C3-C4-C5 | 119.56(13) | 119.74 | 119.75 | 119.79 |
| C4-C5-C6 | 120.59(12) | 120.04 | 120.03 | 120.01 |
| C5-C6-C1 | 120.12(12) | 120.62 | 120.63 | 120.64 |
| C6-C1-C2 | 119.09(13) | 118.96 | 118.93 | 118.91 |
| C5-C6-C1 | 120.12(12) | 120.61 | 120.69 | 120.67 |
| C2-C1-C7 | 119.30(12) | 120.43 | 120.38 | 120.41 |
| C1-C7-N | 112.39(11) | 111.22 | 110.75 | 110.63 |
| C7-N-C8 | 125.98(12) | 127.95 | 127.43 | 127.21 |
| N-C8-S | 124.30(11) | 121.24 | 121.33 | 121.48 |
| N-C8-C9 | 115.07(12) | 116.67 | 116.37 | 116.22 |
| S-C8-C9 | 120.63(10) | 122.09 | 122.29 | 122.31 |
| Dihedral angles (°) | | | | |
| C3-C2-C1-C7 | -177.31 | -179.30 | 179.63 | 179.04 |
| C5-C6-C1-C7 | 177.67 | 179.12 | -179.74 | -179.14 |
| C2-C1-C7-N | -143.31 | -57.62 | -68.52 | -76.21 |
| C6-C1-C7-N | 38.99 | 122.86 | 111.02 | 102.83 |
| C1-C7-N-C8 | -102.16 | 155.76 | 165.24 | 170.78 |
| C7-N-C8-S | -1.87 | 174.90 | 176.40 | 177.21 |
| C7-N-C8-C9 | 177.62 | -5.43 | -3.98 | -2.95 |

**Table 3** Selected band assignments of experimental and calculated IR spectra for N-acetylbenzylamine and N-benzyl-ethanethioamide.

| Frequencies ($cm^{-1}$) | | Assignment |
|---|---|---|
| Experimental | Calculated* DFT/B3LYP 6-311++G(3df,2pd) | |
| | N-acetylbenzylamine | |
| 3294 | 3586 | N-H stretch |
| 3079 | 3193 | C=C-H stretch |
| 1637 | 1743 | C=O stretch |
| 1556 | 1625 | N-H bending |
| 1454 | 1531 | aromatic C=C stretch |
| 1235 | 1347 | N-H bending<br>C-N stretching |
| | N-benzyl-ethanethioamide | |
| 3210 | 3578 | N-H stretching |
| 3007 | 3184 | aromatic C=C stretch |
| 1557 | 1525 | N-H bending |
| 1538 | 1645 | aromatic C=C stretch |
| 1345 | 1110 | C=S stretching |
| 1254 | 1357 | aromatic C-H in plane |

* The calculated frequencies have been scaled by the scaling factor 0.96

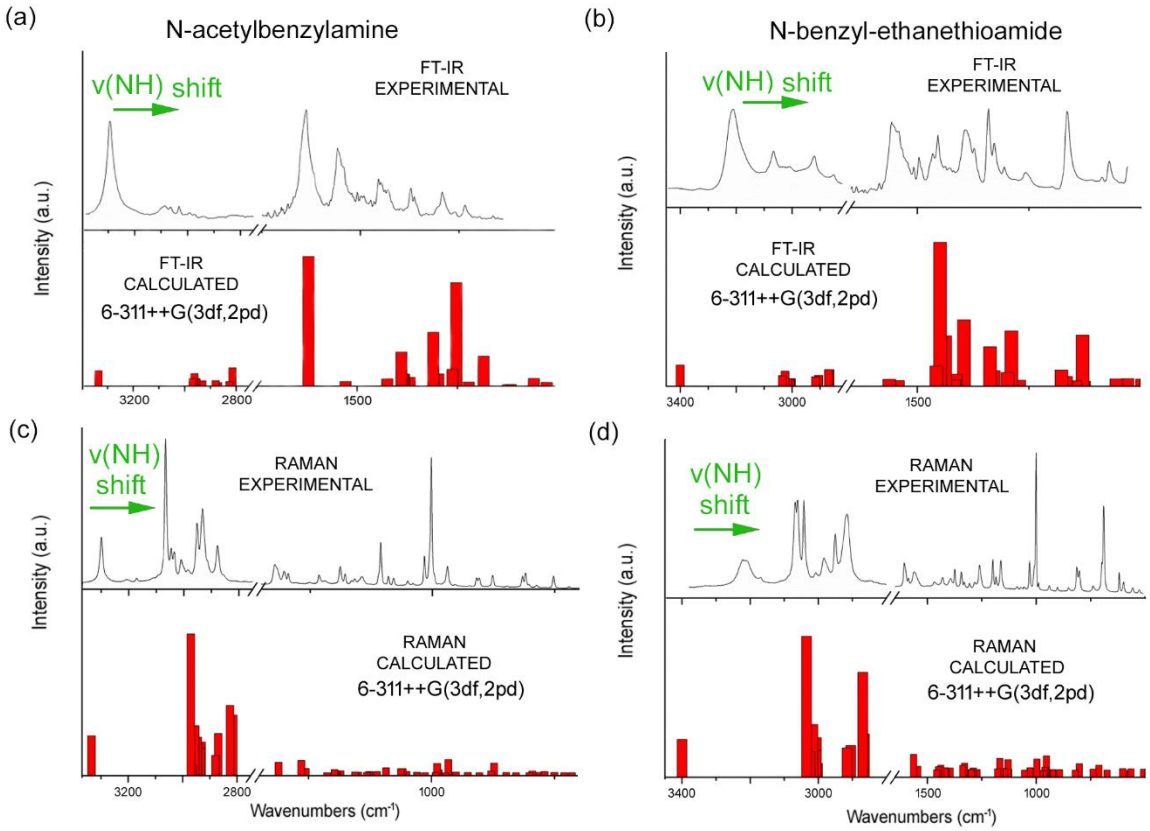


**Fig. 7.** Comparison of B3LYP calculated IR spectrum of N-acetylbenzylamine and N-benzyl-ethanethioamide with the experiment.

### *3.4. Global reactivity descriptors*

As a final point of our investigations, we show the calculated quantum chemical quantities: chemical potential ($\mu$), chemical hardness ($\eta$) and global electrophilicity index ($\omega$). Thus, in order to calculate the quantum chemical descriptors have been used HOMO (highest occupied molecular orbital; represents the ability to donate an electron) and LUMO (lowest unoccupied molecular orbital; represents the ability to obtain an electron) energies. The potential energy difference between the HOMO and LUMO is defined as the HOMO–LUMO energy gap, which reflects the chemical activity of analyzed molecules. The energies of the HOMO and LUMO orbital have been calculated using at the B3LYP/6-311(d,p), B3LYP/6-311++G(d,p) as well as B3LYP/6-311++G(3df,2pd) level and have been shown in Table 4.

The HOMO-LUMO energy diagram of (**1**) and (**2**) obtained by DFT B3LYP/6-311++G(3df,2pd) method has been presented in Fig. 7. Herein, it should be pointed that the HOMO-LUMO energy diagrams obtained in the case of the DFT/B3LYP method with 6-311(d,p) and 6-311++G(d,p) basis set are comparable to the HOMO-LUMO energy diagram received by the 6-311++G(3df,2pd) basis set (data not shown).

**Table 4.** Calculated energies values of N-acetylbenzylamine and N-benzyl-ethanethioamide in gas phase.

| | | DFT/B3LYP | | |
|---|---|---|---|---|
| | | 6-311(d,p) | 6-311++G(d,p) | 6-311++(3df,2pd) |
| N-acetylbenzylamine | HOMO [eV] | -6.72708 | -6.89661 | -7.02478 |
| | LUMO [eV] | -0.60084 | -0.86208 | -0.79840 |
| | $\Delta E_{HOMO\text{-}LUMO\ gap}$ [eV] | 6.126238 | 6.034533 | 6.226378 |
| N-benzyl-ethanethioamide | HOMO [eV] | -5.6884 | -5.69874 | -5.68350 |
| | LUMO [eV] | -1.02644 | -1.17365 | -1.17501 |
| | $\Delta E_{HOMO\text{-}LUMO\ gap}$ [eV] | 4.66196 | 4.525083 | 4.508484 |

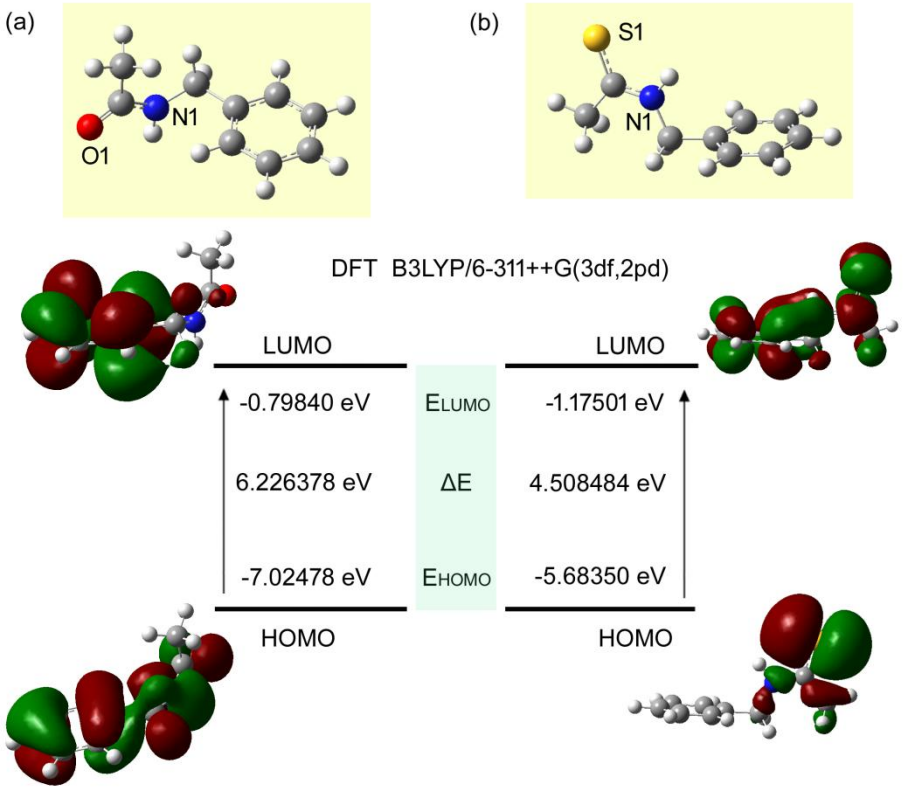


**Fig. 7.** The HOMO-LUMO energy diagram of (a) N-acetylbenzylamine and (b) N-benzyl-ethanethioamide.

As can be seen from the Table 4, the energy barrier $E_{LUMO}$ - $E_{HOMO}$ is higher in the case of N-acetylbenzylamine, while N-benzyl-ethanethioamide is characterized by smaller HOMO–LUMO gap. Herein, it should be also stressed that an electronic system with a larger HOMO‑LUMO gap is less reactive than one having smaller gap. One can add that quantum chemistry calculation reveals that the substitution of –C=O by –C=S group results in a great increase of HOMO energy level, and a great decrease of $\Delta E_{HOMO\text{-}LUMO\ gap}$ obviously.

Finally, the calculated value of the electrophilicity index (a measure of energy lowering due to maximal electron flow between donor and acceptor) of (**1**) and (**2**) is 2.1913 eV (B3LYP/6-311(d,p)), 2.4939 eV (B3LYP/6-311++G(d,p)), 2.4574 eV (B3LYP/6-311++(3df,2pd)) as well as 2.4179 eV (B3LYP/6-311(d,p)), 2.6093 eV (B3LYP/6-311++G(d,p)), 2.6084 eV (B3LYP/6-311++(3df,2pd)), respectively. Thus, it is clearly seen that both compounds are classified as strong electrophiles. It is well known that the $\omega$ describe the biological activity of compounds.

## 4. Conclusions

The results of the spectral measurements (IR and Raman), Hirshfeld Surfaces analysis and DFT quantum chemical calculations have been investigated. The spectral experimental results add new data to the spectroscopy of N-acetylbenzylamine and its sulphur analogue - N-benzyl-ethanethioamide. In the crystal structure of (**1**) and (**2**) molecules are connected by long chains of the N-H···O and N-H···S hydrogen bonds, respectively. Additionally, the H···H and C···H intermolecular interactions have an important influence on the stabilization of the crystal lattice packing of both compounds, and which characterize clear signatures in the 2D fingerprint plots. Combination of spectroscopic and theoretical analysis enabled us to conclude, that forming the hydrogen bonds (N-H···O and N-H···S) shift the $\nu_{N\text{-}H}$ bands towards lower frequencies. In fact, the IR spectroscopy in polarized light of hydrogen-bonded

molecular crystals is able to provide crucial experimental data in the area of the hydrogen bond research. Further, the temperature effect is very important and useful, because it differentiates the properties of the shorter-wave band branches from the longer-wave ones in the case of (**1**) and (**2**). We believe that the information on the hydrogen bonding abilities of the title amide and thioamide will be helpful in understanding the selected biochemical processes.

It was shown that the calculated geometrical parameters, using of B3LYP/6-311(d,p), B3LYP/6-311++G(d,p) and B3LYP/6-311++G(3df,2pd) level, are in good agreement with the experimental values obtained from the crystallographic data. All the vibrational wavenumbers are calculated and scaled values (with 6-311++G(3df,2pd) basis set) are compared with experimental IR and Raman spectra. Experimentally observed frequencies are in good agreement with the calculated values. It has been also shown that the analysis of the Hirshfeld surface is well correlated to the spectroscopic studies.

As a final point, we made calculations the HOMO–LUMO energy gap at the B3LYP/6-311(d,p)/6-311++G(d,p)/6-311++(3df,2pd) level reveals the chemical activity of the molecule. The calculated HOMO and LUMO energies can be used to semiquantitatively estimate not only the electrophilicity index and chemical potential but also electronegativity, chemical hardness or global softness. Besides, it should be pointed that the concepts of electrophilicity of organic molecules are very important for almost all chemists.

**Acknowledgement** Calculations have been carried out using resources provided by Wrocław Centre for Networking and Supercomputing (http://wcss.pl), grant No. 95.

**Conflict of Interest** The authors declare that they have no conflict of interest.

## References

[1] R.S. Fisher, C. Acevedo, A. Arzimanoglou, A. Bogacz, J.H. Cross, Ch.E. Elger, J.E. Jr, L. Forsgren, J.A. French, M. Glynn, D.C. Hesdorffer, B.I. Lee, G.W. Mathern, S.L. Moshé, E. Perucca, I.E. Scheffer, T. Tomson, M. Watanabe, S. Wiebe, A practical clinical definition of epilepsy, Epilepsia. 55 (2014) 475-482.

[2] WHO/IBE/ILAE Global Campaign Against Epilepsy. Atlas epilepsy care in the world, programme for neurological diseases and neuroscience department of mental health and substance abuse, Geneva: World Health Organization. http://www.who.int/entity/mediacentre/factsheets/fs999/en, 2009, (accessed 4 December 2017).

[3] B.J. Steinhoff, Pregnancy, epilepsy, and anticonvulsants, Dialogues Clin Neurosci. 1 (2008) 63-75.

[4] K.R. Scott, Anticonvulsants, in: D.J. Abraham (Eds.), Burger's Medicinal Chemistry and Drug Discovery, Volume 6: Nervous System Agents, Jones Wiley & Sons. Inc., Virginia, 2003, pp. 263-320.

[5] B. Malawska, Application of Pharmacophore Models for the Design and Synthesis of New Anticonvulsant Drugs, Mini-Reviews in Med. Chem. 3 (2003) 341-348.

[6] B. Malawska, K. Kulig, A. Śpiewak, J.P. Stables, Investigation into new anticonvulsant derivatives of α-substituted N-benzylamides of γ-hydroxy- and γ-acetoxybutyric acid. Part 5: Search for new anticonvulsant compounds, Bioorg Med Chem. 12 (2004) 625-632.

[7] S.N. Pandeya, A.S. Raja, J.P. Stables, Synthesis of isatin semicarbazones as novel anticonvulsants – role of hydrogen bonding, J Pharm Pharmaceut Sci. 5 (2002) 266-271.

[8] H. Kohn, J.D. Conley, J.D. Leander, Marked stereospecificity in a new class of anticonvulsants, Brain Res. 457 (1988) 371-375.

[9] P.N. Patsalos, B.F.D. Bourgeois, The Epilepsy Prescriber's Guide to Antiepileptic Drugs, Cambridge University Press, New York, 2010.

[10] Y. Xiao, M. Luo, J. Wang, H. Luo, Losigamone add-on therapy for partial epilepsy, Cochrane Database of Syst Rev. 12 (2015) 1-40.

[11] S.P. Aiken, W.M. Brown, Treatment of epilepsy: existing therapies and future developments, Front Biosci. 5 (2000) 124-152.

[12] V. Kathuria, D.P. Pathak, Synthesis and anticonvulsant activity of some N-substituted-phthalimide analog, J Pharm Innov. 1 (2012) 55–59.

[13] M.G. Wong, J.A. Defina, P.R. Andrews, Conformational Analysis of Clinically Active Anticonvulsant Drugs, J. Med. Chem. 29 (1986) 562-572.

[14] Y. Maréchal, The Hydrogen Bond and the Water Molecule, Elsevier, 2007.

[15] S. Winiwarter, M. Ridderström, A.L. Ungell, T.B. Andersson, I. Zamora, Use of Molecular Descriptors for Absorption, Distribution, Metabolism, and Excretion Predictions, in: J.B. Taylor, D.J. Triggle (Eds.) Comprehensive Medicinal Chemistry II, Volume 5: ADME-Tox Approaches, Elsevier, Amsterdam, 2007, pp. 531-554.

[16] H. Tan, W. Qu, G. Chen, R. Liu, The Role of Charge Transfer in the Hydrogen Bond Cooperative Effect of cis-N-Methylformamide Oligomers, J. Phys. Chem. A. 109 (2005) 6303-6308.

[17] C. Béguin, A. LeTiran, J.P. Stables, R.D. Voyksner, H. Kohn, N-Substituted amino acid N'-benzylamides: synthesis, anticonvulsant, and metabolic activities, Bioorg. Med. Chem. 12 (2004) 3079-3096.

[18] R. Vardanyan, V. Hruby, Antimicrobial Drugs, in Synthesis of Essential Drugs, Elsevier, Amsterdam, 2006, pp. 499-524.

[19] Ho-Jin Lee, Young-Sang Choi, Kang-Bong Lee, Jeunghee Park, and Chang-Ju Yoon, Hydrogen Bonding Abilities of Thioamide, J. Phys. Chem. A, 106 (30) (2002) 7010–7017.

[20] W. Śmiszek-Lindert, J. Kusz, N-benzylacetamide, Acta Cryst. Sec. E. E63 (2007) o3713.

[21] W. Śmiszek-Lindert, O. Lindert, M. Nowak, J. Kusz, 3'-Methylacetanilide and N-benzylthioacetamide at low temperature, Acta Cryst. Sec. C. C64 (2008) o599-o603.

[22] H.T. Flakus, W. Śmiszek-Lindert, K. Stadnicka, Strong vibronic coupling effects in polarized IR spectra of the hydrogen bond in N-methylthioacetamide crystals, Chem. Phys. 335 (2007) 221–232.

[23] H.T. Flakus, W. Śmiszek-Lindert, B. Hachuła, A. Michta, H/D isotopic recognition mechanism in hydrogen-bonded crystals of 3-methylacetanilide and 4-methylacetanilide, Spectrochim. Acta, Part A. 97 (2012) 263–273.

[24] H.T. Flakus, W. Śmiszek-Lindert, B. Hachuła, H/D Isotopic Recognition in Hydrogen-Bonded Systems: Strong Dynamical Coupling Effects in the Polarized IR Spectra of 3-Methylthioacetanilide and 4-Methylthioacetanilide Crystals, J. Phys. Chem. A 115 (2011) 7511–7520.

[25] W.E. Śmiszek-Linderta, E. Chełmecka, S. Góralczyk, M. Kaczmarek, Vibrational spectroscopic (FT-IR, FT-Raman) studies, Hirshfeld surfaces analysis, and quantum chemical calculations of m-acetotoluidide and m-thioacetotoluidide, J. Mol. Struct. 1128 (2017) 619-628.

[26] W. Śmiszek-Lindert, A. Michta, A. Tyl, G. Małecki, E. Chełmecka, S. Maślanka, X-Ray, Hirshfeld surface analysis, spectroscopic and DFT studies of polycyclic aromatic hydrocarbons: fluoranthene and acenaphthene, J. Serb. Chem. Soc. 80 (2015) 1489–1504.

[27] J. Toporski, T. Dieing, O. Hollricher, Confocal Raman Microscopy. In Optical Sciences, Springer, Berlin, Germany, 2011.

[28] S.K. Wolff, D.J. Grimwood, J.J. McKinnon, D. Jayatilaka, M.A. Spackamn, Crystal Explorer 3.0 University of Western Australia, Perth, 2007.

[29] C. Lee, W. Yang, R.G. Parr, Development of the Colle-Salvetti correlation-energy formula into a functional of the electron density, Phys Rev B. 37 (1998) 785–789.

[30] A.D. Becke, Density- functional thermochemistry. III. The role of exact exchange, J. Chem. Phys. 98 (1993) 5648–5652.

[31] Gaussian 09, Revision A.02, M.J. Frisch, G.W. Trucks, H.B. Schlegel, G.E. Scuseria, M.A. Robb, J.R. Cheeseman, G. Scalmani, V. Barone, B. Mennucci, G.A. Petersson, H. Nakatsuji, M. Caricato, X. Li, H.P. Hratchian, A.F. Izmaylov, J. Bloino, G. Zheng, J.L. Sonnenberg, M. Hada, M. Ehara, K. Toyota, R. Fukuda, J. Hasegawa, M. Ishida, T. Nakajima, Y. Honda, O. Kitao, H. Nakai, T. Vreven, J.A. Montgomery, J.E. Peralta, F. Ogliaro, M. Bearpark, J.J. Heyd, E. Brothers, K.N. Kudin, V.N. Staroverov, R. Kobayashi, J. Normand, K. Raghavachari, A. Rendell, J.C. Burant, S.S. Iyengar, J. Tomasi, M. Cossi, N. Rega, J.M. Millam, M. Klene, J.E. Knox, J.B. Cross, V. Bakken, C. Adamo, J. Jaramillo, R. Gomperts, R.E. Stratmann, O. Yazyev, A.J. Austin, R. Cammi, C. Pomelli, J.W. Ochterski, R.L. Martin, K. Morokuma, V.G. Zakrzewski, G.A. Voth, P. Salvador, J.J. Dannenberg, S. Dapprich, A.D. Daniels, O. Farkas, J.B. Foresman, J.V. Ortiz, J. Cioslowski, Fox DJ Gaussian Inc., Wallingford CT, 2009.

[32] L. Shu-Bin, Conceptual Density Functional Theory and Some Recent Developments, Acta Phys Chim Sin. 25 (2009) 590–600.

[33] P. Geerlings, F. De Proft, W. Langenaeker, Conceptual density functional theory, Chem Rev. 103 (2003) 1793–1873.

[34] R.G. Parr, W. Yang, Density functional theory of atoms and molecules, Oxford University Press, NewYork, 1989.

[35] R.G. Pearson, Chemical Hardnesss Applications from Molecules to Solids, VCH-Wiley, Weinheim, 1997.

[36] R.G. Parr, L.V. Szentpaly, S.J. Liu, Electrophilicity Index, Am Chem Soc. 121 (1999) 1922–1924.

[37] W. Kohn, L. Sham, Self-Consistent Equations Including Exchange and Correlation Effects, J Phys Rev. 140 (1965) 1133–1138.

[38] H.T. Flakus, A. Michta, Strong coupling effects in the polarized IR spectra of the chain hydrogen bond systems in imidazole crystals: H/D isotopic 'self-organization' effects in the IR spectra of isotopically diluted imidazole single crystals, J Mol Struct. 707 (2004) 17–31.

[39] S.K. Seth, G.Ch. Maity, T. Kar, Structural elucidation, Hirshfeld surface analysis and quantum mechanical study of para-nitro benzylidene methyl arjunolate, J Mol Struct. 1000 (2011) 120–126.

[40] H.D. Holtje, M. Hense, S. Marrer and E. Maurhofer, The use of quantum chemical methods to study molecular mechanisms of drug action in Progres in Drug Research, Vol 34, Edited Ernst Jucker, Basel, 1990, pp. 9-68.

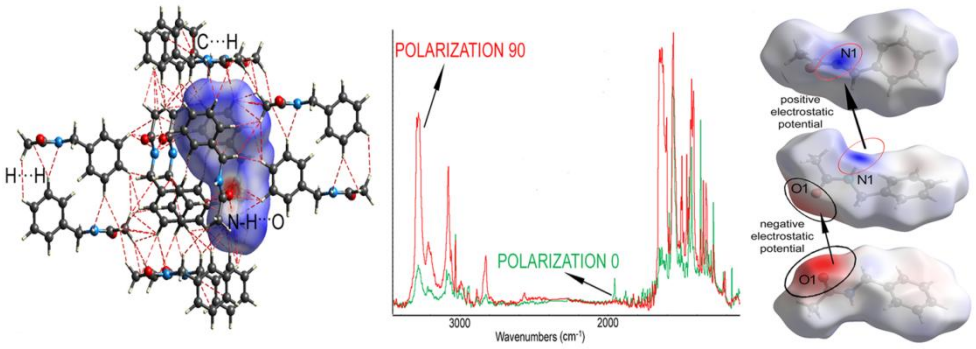


Graphical abstract

**Highlights**

· IR and Raman investigations (experimentally and theoretically) were carried out

· The polarized IR spectra of the hydrogen bond in crystals of amide and thioamide were studied

· Hirshfeld surfaces analysis and DFT studies have been reported

· The HOMO–LUMO energy gap was theoretically predicted.